Central European Journal of Energetic Materials, **2014**, *11*(3), 417-431
ISSN 2353-1843

A Novel, Non-invasive Method for the Detection of Combustion Zone Propagation in Solid High Energy Materials by Means of Thermocouples and Pyrolytic Graphite

Maciej MISZCZAK[1*], Waldemar ŚWIDERSKI[1],
Andrzej Jarosław PANAS[2]

[1]*Military Institute of Armament Technology,*
7 Wyszyńskiego St., 05-220 Zielonka, Poland
[2]*Faculty of Mechatronics and Aerospace,*
Military University of Technology,
2 Kaliskiego St., 00-908 Warsaw, Poland
[*]*E-mail: mpf.miszczak@op.pl*

Abstract: This work presents a new, non-invasive method for the discrete detection of combustion zone propagation in high energy materials – pyrotechnic compositions – by means of thermocouples bonded to the external, side surface of a pyrolytic graphite (pyrographite) tube filled with the pyrotechnic composition and ignited at the one end by a CO_2 laser. The thermocouples were positioned in a line parallel to the longitudinal axis of the pyrographite tube, which was used as a directional heat guide (thermal management) and a thermoresistant structure, enabling detection of the propagation of the combustion zone as a heat zone generated by the combustion, traveling on the outside surface of the pyrographite tube along its axis. Such a directional heat guidance was caused by the unique thermal conductivity anisotropy of pyrographite resulting in low thermal conductivity of the pyrographite tube along its axis and high thermal conductivity across the tube radius. The thermocouples detected passages of the outside heat zone that were equally time delayed in relation to the combustion zone inside the tube. Dividing the distance between the thermocouples by the time between their thermoelectric response to the same (corresponding) isotherm of the heat zone, gave the average burning rate of the high energy composition being tested over the distance between the thermocouples. The proposed procedure for burning rate determination was verified by numerical simulations.

Keywords: solid high energy materials, combustion zone propagation, average burning rate, thermocouples, pyrolytic graphite (pyrographite)

1 Introduction

Thermocouples are commonly used as intrusive gauges installed in solid high energy materials for registration of the temperature profile of the combustion zone/front, sometimes with the option for measurement of the average burning rate over the distance between the thermocouples [1-9]. Optionally, thermocouples may be mounted on the outside of high energy materials to measure the temperature distribution on/through the walls of rocket motors, including their combustion chambers and nozzles [10-13]. When the thermocouples are in direct contact with the high energy charge, they introduce foreign bodies in its structure, discontinuities which disturb to the certain degree the combustion process of the high energy charge. From the moment when the combustion zone reaches the positions of the thermocouples, they are exposed to the severe action of combustion products due to their high temperature and/or pressure and/or flow. Another disadvantage of the use of thermocouples is connected with the inconvenience in mounting them directly in the high energy charge.

The idea of applying thermocouples as non-intrusive gauges to detect combustion zone propagation emerged during tests on the detection by IR thermal camera of combustion zone propagation in end-burning, solid high energy materials (homogeneous and heterogeneous) inserted into tubes made of pyrolytic graphite (pyrographite) and ignited from one end by a laser [14-16]. The observed heat zone, induced on the external side surface of the pyrographite tube by the combustion zone, travelled from the ignition end to the opposite end of the tube successively reaching its basal crystallographic planes (layers). Visualization of the combustion zone propagation as an external heat zone was possible due to the contact of the tested high energy material with the pyrolytic graphite. Another obligatory requirement in successfully performing the above visualization, relied on the appropriate orientation of the pyrographite crystallographic basal planes in relation to the direction of propagation of the combustion zone/front, *i.e*. across this direction, ideally perpendicular to it.

2 Experimental

2.1 Materials and measurement arrangement

For the tests, cylindrical, end-burning, pressed pyrotechnic charges in the form of cylindrical columns of a low-gas delay composition based on the oxidizers barium chromate and potassium chlorate(VII), with a nominal burning rate covering the range 1.2-1.5 mm/s under standard pressure and temperature conditions, were

selected. The above mentioned pyrotechnic compositions are commonly used in self-destructing elements of ammunition, especially in artillery and rocket fuses.

The pyrotechnic sample to be tested was inserted into the pyrographite tube, total length 16.7 mm, consisting of three pyrographite rings of length 6.0, 4.7 and 6.0 mm, starting from the ignition end to burn out end. The lengths of the sample and the tube were the same. The tube had internal and external diameters of 5.2 mm and 14.4 mm, respectively. Each pyrographite ring had density 2.18 g/cm^3, measured by gas-pycnometry, which is the appropriate apparatus because of the extremely low gas permeability of pyrographite. These results were confirmed later by hydrostatic density measurements performed on pyrolitic graphite test specimens. The density measured by the latter method was 2.182 g/cm^3. The density value obtained is in compliance with literature data and confirms to a certain extent the satisfactory quality of the pyrographite crystallographic structure on a macro scale. The pyrographite rings were bonded to each other through their end surfaces by a thermoresistant adhesive which could withstand temperatures up to 200 °C. The cylindrical surface of the tested charge was bonded to the inner wall of the pyrographite tube by a thin layer of adhesive [2 wt.% solution of nitrocellulose lacquer in a mixture of ethyl acetate and acetone (1/1) (v/v)] in order to prevent flow of the combustion products between the surface of the tube and the unconsumed (unburnt) part of the charge.

Pyrographite exhibits an anisotropic thermal conductivity ranging over about two orders of magnitude depending on the direction of heat propagation, *i.e*. parallel to the planar crystallographic layers (a,b) or perpendicular (c) to them. In our case the pyrographite tube had a very high radial thermal conductivity, whilst its axial component was quite low. The ratio of radial to axial thermal conductivity was estimated to be more than 80 on the basis of previous experimental investigations [17]. In order to confirm the above estimate of the thermal conductivity anisotropy of the tested pyrographite, the following experimental investigations were conducted.

The pyrographite thermal conductivity had been determined, together with other thermophysical properties such as heat capacity and thermal diffusivity, in the course of some complementary measurements. The thermal conductivity was calculated from the density, heat capacity, and the thermal diffusivity data. The additional density measurements had been performed on a microbalance applying hydrostatic weightings at room temperature. The heat capacity had been obtained using a Perkin-Elmer Pyris 1 differential scanning calorimeter. The procedure of these experimental studies were the same as described in [18] and [19]. Owing to anisotropy in the transport properties of the material, the thermal diffusivity measurements appeared to be the most demanding ones. After several

studies it was eventually decided to apply the temperature oscillation method [20]. The main investigations had been done on pyrographite cuboid specimens of dimensions 40×40×4 mm. The direction (c) parallel to the shortest cuboid edge, is the one of low thermal conductivity and the directions (a,b) parallel to the longer edges, are of high thermal conductivity. Two different configurations of the measurement system were applied in order to study the "propagation" of periodic temperature changes in the two characteristic directions, *i.e*. of low or high thermal conductivity. In both cases the temperature changes were measured by tiny thermocouples attached to the opposite cuboid sides. This means that the thermal diffusivity obtained corresponds to the bulk value of this parameter. Certain studies performed with remote IR temperature measurements revealed much higher local thermal conductivity values in the planar crystallographic directions than in the direction perpendicular to the crystallographic planes; the details are presented in [17]. However, these data have been excluded from the present studies. In conclusion, the acquired representative values of the thermophysical properties of pyrographite and the calculated thermal conductivity data are provided in Table 1. The ratio of the thermal conductivity in the radial to the axial direction of the pyrographite tube is equal to about 56, from the thermocouple data (oscillation method [20]), and about 160 from the infrared studies [17]. It is worth mentioning here that the latter values for the ratio of thermal conductivities are relatively comparable with data reported in references [13, 21] for the pyrolytic graphite used in solid propellant rocket motors.

Table 1. Thermophysical properties of pyrographite at room temperature (20 °C) obtained from experimental investigations

Direction	Density [kg·m^{-3}]	Heat capacity [J·kg^{-1}·K^{-1}]	Thermal diffusivity [mm^2·s^{-1}]	Thermal conductivity [W·m^{-1}·K^{-1}]
(a,b) / radial	2180	698	62.8	99
(c) / axial			1.15	1.76

Utilizing the experimental arrangement presented in Figure 1, the high energy charge inserted into the pyrographite tube was ignited at one end by a CO_2 laser beam of wavelength 10.6 μm and power 7.0 W, which was cut off when ignition commenced. The optical configuration of the laser lenses and the length between the output head of the laser and the ignited surface of the high energy charge, which was 800 mm, caused the laser beam to cover an area of 3.0 mm diameter on the head surface of the high energy charge being tested. Two K-type NiCr-Ni thermocouples were bonded to the external, side surface of

the pyrolytic graphite (pyrographite) tube by means of high temperature epoxy adhesive, which was able to withstand temperatures up to 200 °C. The contact points of the thermocouples with the pyrographite surface formed a line parallel to the longitudinal axis of the pyrographite tube.

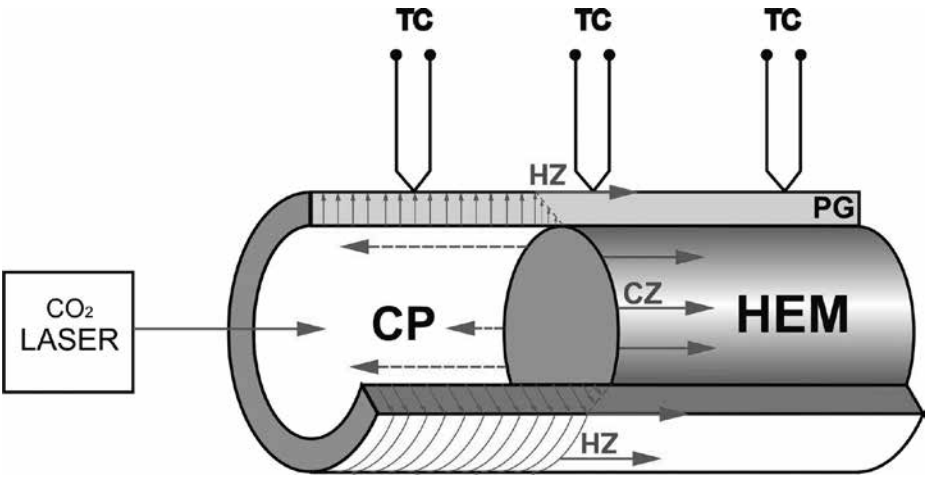

Figure 1. Schematic diagram of an example of the experimental setup consisting of thermocouples (TC) for the detection of the propagation of the heat zone (HZ) on the external surface of the pyrographite (PG) tube. The heat zone (HZ) is generated by the combustion zone (CZ) during burning of solid high energy material (HEM) ignited by a CO_2 laser beam. CP – combustion products of HEM.

2.2 Test results and discussion

The temperature-time profiles of the thermoelectric responses of the two thermocouples during and after the burning of the low-gas pyrotechnic composition are presented in Figure 2.

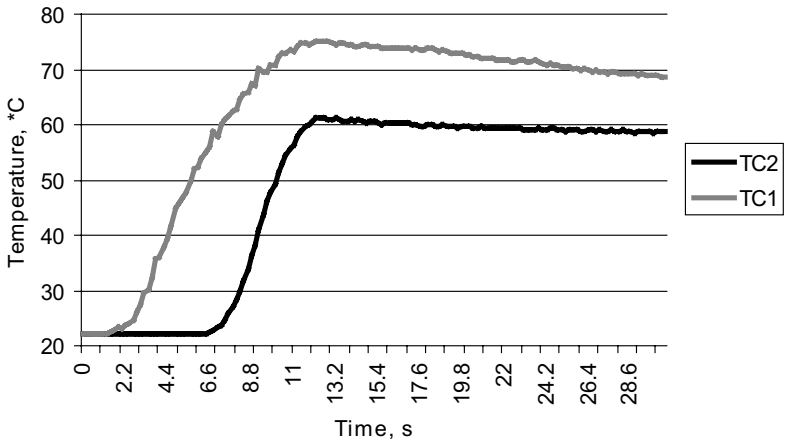

Figure 2. Example of the temperature-time profiles obtained during and after the burning of the pyrotechnic, low-gas delay composition on the basis of oxidizers − barium chromate and potassium chlorate(VII), illustrating the subsequent responses of two thermocouples (TC1, TC2) to the passage of the heat zone, bonded to the external surface of the pyrographite tube, 16.7 mm long, at the distances of 5.0 mm from the initiation end of the tube and 5.0 mm from opposite end of the tube, resulting in a distance of 6.7 mm between the thermocouples (TC1, TC2).

The thermocouples were situated 5.0 mm from each end of the pyrographite tube (high energy charge) resulting in a distance of 6.7 mm between them. The thermocouples detected the passage of the heat zone on the external side surface of the tube. The position of this external heat zone was delayed in relation to the combustion zone (Figure 1). When the heat zone passed the contact point of each thermocouple, the temperatures registered by the thermocouple started to increase, and when the high energy material was burnt out, the registered temperatures started to decrease (Figure 2). The maximum temperature registered by the thermocouple located closest to the initiation end of the pyrographite tube, *i.e*. being the first to be exposed to the heat impact from the combustion products, was higher than the maximum temperature registered by the second thermocouple situated farther from the initiation end. The maximum temperature measured by the first thermocouple, being exposed longer to the thermal stimulus of the combustion products, did not exceed 80 °C, and the maximum temperature registered by the second thermocouple was a little over 60 °C. The time corresponding to the maximum values of the temperature response of each

thermocouple, *i.e*. corresponding to the end of burn of the high energy charge, was the same for each thermocouple.

For a more precise determination of the period between the responses of the thermocouples, in order to determine the average burning rate of the high energy charge being tested, Figure 3 is more suitable because it shows at a larger scale the initial increasing part of the temperature responses of the thermocouples.

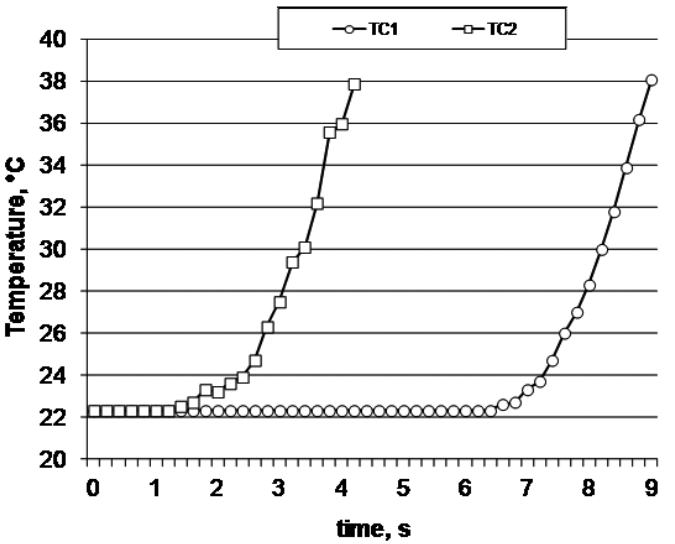

Figure 3. Enlarged initial part of the temperature responses of the thermocouples (TC1, TC2) taken from Figure 2.

Dividing the distance between the thermocouples by the time between their thermoelectric responses to the same (corresponding) isotherm of the heat zone, *e.g*. 30 °C, which was 4.8 s, it is possible to determine the average burning rate of the high energy composition over the distance between the thermocouples, which was 1.40 mm/s for this example, presented in Figures 2 and 3. For the next three firings of the same type of pyrotechnic sample, under identical experimental conditions using the same arrangement, *i.e*. the same pyrographite tube with the same configuration of the thermocouples, the average burning rates obtained were: 1.34, 1.28 and 1.38 mm/s.

In order to test the above non-intrusive thermocouple method, numerical modelling was applied as described below.

3 Numerical modeling

The proposed procedure for the determination of the burning rate of high energy material has been examined by numerical simulation. During the tests performed, both metrological conditioning and the performance of the method have been evaluated. The numerical studies were done using Comsol/M FEM software [22]. The analysis focused mostly on heat conduction within the pyrographite tube. Due to the relatively low thermal conductivity of the material of the pyrotechnic charge in comparison with the pyrographite thermal conductivity, heat conduction within the charge insert was excluded from consideration. The 2D axially-symmetric heat conduction problem seems to reflect reasonably well a real cylindrical configuration of the pyrotechnic charge in the tube. The scheme of the developed geometrical model is shown in Figure 4.

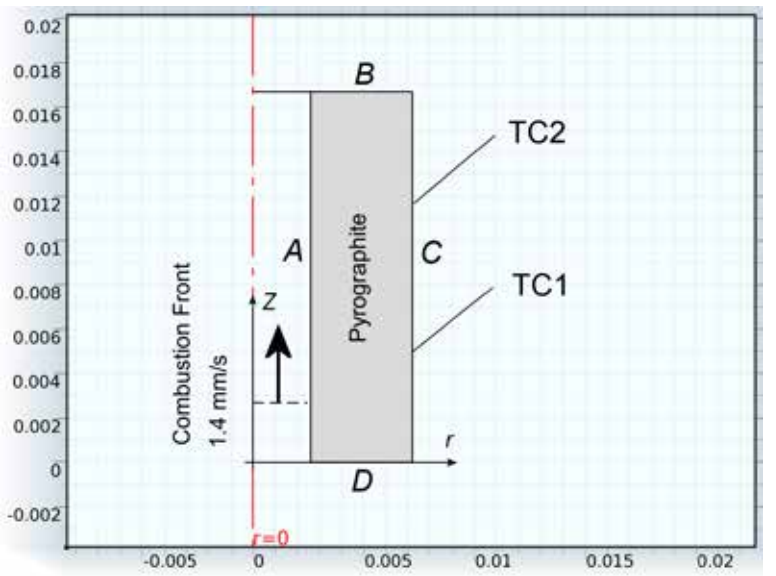

Figure 4. Scheme of the 2D axially symmetric model of the sensoric pyrographite tube structure: *A* – internal boundary, *B, C, D* – external boundaries, TC1 and TC2 – thermocouple sensor locations.

The thermal properties of the pyrographite tube were assumed to be independent of temperature and equal to the values displayed in Table 1. Therefore, the modelling problem falls into the partial differential Fourier equation of transient heat transfer [23] with adequate initial and boundary conditions. Because of the attention focused on the directional heat transfer

within the anisotropic pyrographite tube, it was believed that the accepted model represents the observed phenomena.

For the calculations, a uniform initial condition of a temperature equal to 20 °C was taken. All four boundaries *A*, *B*, *C* and *D* (Figure 4) were subjected to the convective heat transfer condition. In addition, radiative heat loss into the surroundings at 20 °C from boundaries *B*, *C* and *D* was assumed. The convective heat transfer coefficient for boundary *C* was evaluated by applying the appropriate criteria formulae for an infinite tube of the appropriate diameter [24]. The same value was assumed for boundaries *B* and *D*. The boundary condition parameters discussed above are listed in Table 2.

For the numerical simulation, a burning rate of the pyrotechnic charge of 1.40 mm·s^{-1} was assumed. This burning rate corresponds to a burning time of 11.929 s. Within the time interval from 0 to 11.929 s, the combustion front propagation was modelled by varying the spatial distribution of the heat transfer coefficient at boundary *A* (an inner cylindrical tube surface as illustrated in Figure 5).

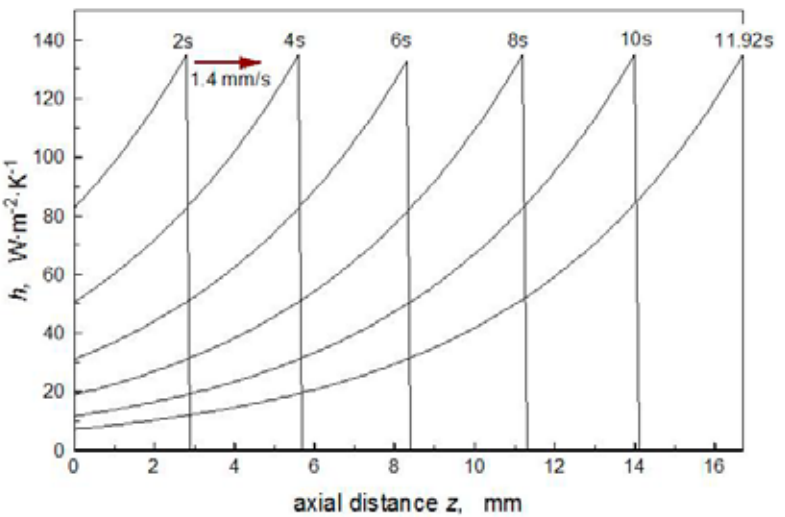

Figure 5. Axial distribution of the heat transfer coefficients at the indicated stages of the modelled combustion process – illustration of the propagation of the combustion front along the internal wall *A*.

The appropriate formula describing the heat transfer coefficient profile is as follows:

$$h(z,\tau) = 135 \exp[175(z - 0.0014\tau)] \quad (1)$$

For time greater than 11.929 s the value of the heat transfer coefficient was switched to 0, meaning thermal insulation, *i.e*. adiabatic conditions at the *A* boundary. The temperature of the combustion products was assumed to be equal to 1700 °C. The parameters of the boundary condition exponential function: the amplitude and decay parameters, were taken as shown in Equation 1 in order to match the simulation result to the experimental profile of the temperature changes as shown in Figure 2. It should be stressed that these particular data, even when taken arbitrarily, did not significantly affect the result of the final analysis, which was identification of the modeled burning rate from the temperature histories from TC1 and TC2 (see Figure 4).

Table 2. Parameters for the boundary conditions assumed for numerical simulation

Boundary / Time interval n.a. / [s]	Heat transfer coefficient [W·m^{-2}·K^{-1}]	External temperature [°C]	Radiation type n.a.	Surface emissivity n.a.	Ambient temperature [K]
A / $0 \leq \tau < 11.929$	Eq. 1	20	None	n.a.	n.a.
A / $11.929 \leq \tau$	0	n.a.	None	n.a.	n.a.
B, *C* and *D*	8	20	Surface to ambient	0.98	293.15

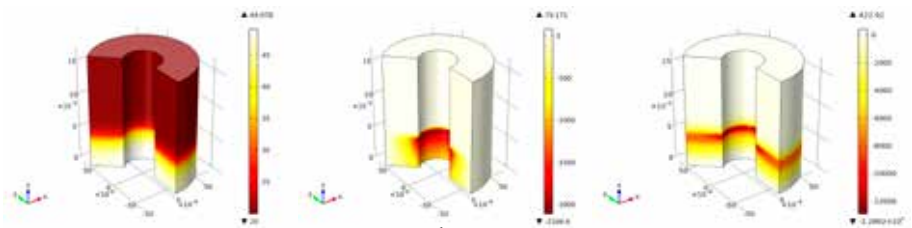

a b c

Figure 6. Simulated 3D images of: a − the temperature distribution (scale 20-49.078 °C), b – radial temperature gradient (scale -2106.6-79.171 K·m^{-1}), and c – axial temperature gradient (scale -12892-422.92 K·m^{-1}) within the pyrographite tube, at 3.55 s of combustion process for all of the above cases (a, b, c).

Prior to the calculations, the domain of the pyrographite was meshed by applying quadrilateral elements. The mesh density was defined by 20 elements in the radial direction and the same (20 elements) in the axial dimension. The final calculations were performed within the time interval 0-30 s, applying a fixed time interval of 0.05 s.

Typical results from a numerical simulation are shown in Figure 6.

The pictures shown in Figure 6 illustrate the temperature and the temperature gradient distribution at $\tau = 3.55$ s, this being the time when the combustion front passes the axial coordinate of the TC1 position. Analysis of these "frame" images provides qualitative proof for the proper functioning of the anisotropic pyrographite tube in transferring the temperature data from the inner cylindrical surface to the outside one.

A quantitative analysis was performed on the temperature histories taken from the TC1 and TC2 locations (Figure 4) that correspond to the thermocouple sensors locations in real experiments (compare previous section). The appropriate time curves are shown in Figure 7.

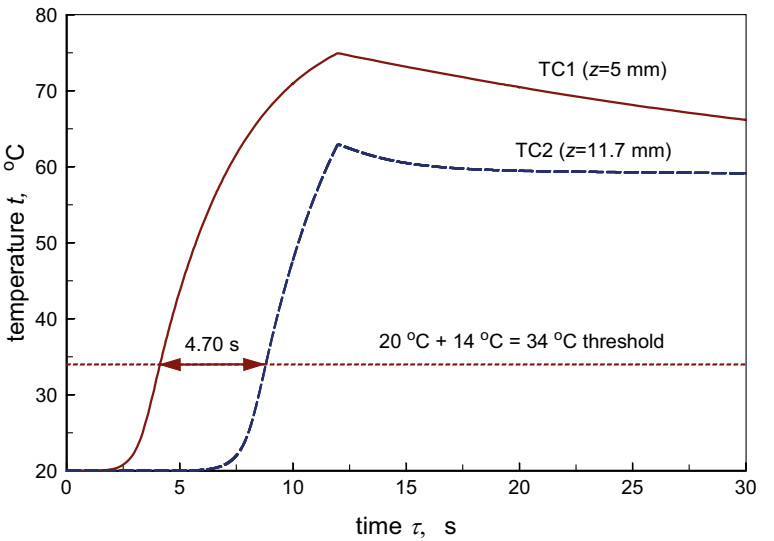

Figure 7. Temperature histories from TC1 and TC2 for numerical simulation at a burning rate of 1.4 mm·s^{-1}.

In the first stage of the processing of the numerical data, the modelled burning rate was obtained in a manner analogous to the experimental procedure, *i.e.* from the 14 °C temperature rise threshold data. By dividing the distance between TC1 and TC2, 6.7 mm, by the time interval corresponding to the appropriate times of the passing threshold, one can easily obtain the burning rate. The result obtained agrees with the data assumed for the numerical simulation within 2% (compare Table 3). However, because of the arbitrarily chosen threshold value, this method could raise some doubts. To avoid any controversy, a second procedure for burning rate evaluation from the recorded temperature histories has been tested.

In this case, the time interval corresponding to the appropriate points has been obtained as the time between the temperature rise inflexion points (Figure 8).

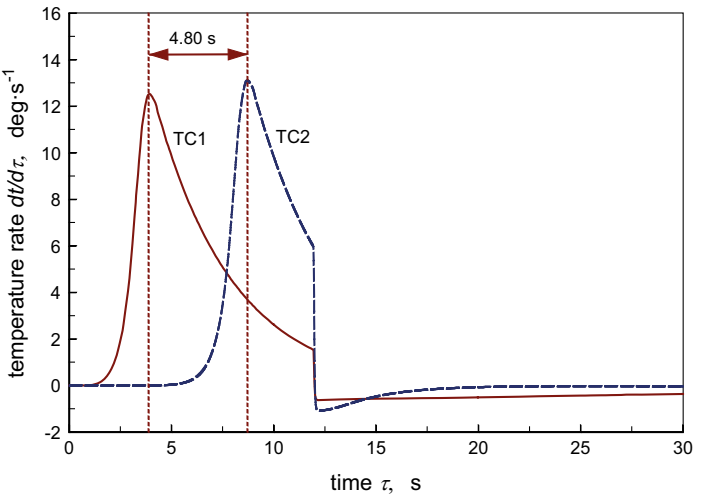

Figure 8. Temperature change rates at TC1 and TC2 from numerical simulation, with an indication of the procedure for identification of the temperature inflexion point from its first derivative.

This is equivalent to the evaluation of the distance between the maxima of the temperature derivatives with respect to time, as shown in Figure 7. The results obtained from the temperature – time histories presented in Figures 7 and 8, and collected in Table 3, are more than satisfactory. They are in very good compliance. It should be mentioned that the performance of this second procedure has been confirmed in additional simulations.

Table 3. Results of the "burning rate" identification from TC1 and TC2 temperature histories obtained in the course of the numerical simulations

Method	Illustration	Burning rate [mm·s^{-1}]	Relative difference [%]
14 °C temperature rise threshold	Fig. 7	1.4255	1.82
Temperature rise inflexion point	Fig. 8	1.3958	-0.30

4 Conclusions

On the basis of the experimental measurements presented and our observations, it is possible to come to the following conclusions:

Non-invasive detection of combustion zone propagation during the burning of high energy charges by the thermocouples, is ensured if the following criteria are fulfilled:

- direct contact of the side surface of the high energy end-burning charge with the inner, side surface of the pyrographite tube, *i.e*. with its inner surface of high heat transfer coefficient;
- adjustment (orientation) of the parallel, crystallographic basal planes of the pyrographite tube in relation to the direction of combustion zone propagation, according to which, these basal planes are situated across this direction, *i.e*. perpendicularly;
- constant thickness of the pyrographite tube wall and the bonding (adhesive) layer between the high energy material and the inner surface of the pyrographite tube being as thin as possible, ensuring maintenance of a constant spatial/time shift for heat delivery by the combustion zone to the point of contact of the thermocouple with the tube;
- direct contact of the thermocouples with the external, side surface of the pyrographite tube, *i.e*. with its outer surface of high heat transfer coefficient;
- contact points of the thermocouples forming a line parallel to the pyrographite tube axis.

Application of a pyrographite tube as a thermal management (heat guiding) structure and a highly thermoresistant barrier of relatively high wall thickness, with very high heat transfer efficiency along the radial direction towards the external, cylindrical side surfaces, and with relatively high heat capacity, resulted in relatively low temperature responses of the thermocouples to high temperature flow fields of the combustion products being obtained. The thermocouples were exposed only to relatively low thermal stresses during the combustion process, which did not caused their degradation or destruction. Because the thermocouples were not exposed directly to the severe impact of the flow of combustion products, much less thermoresistant thermocouples can be utilized instead of highly thermoresistant ones.

This means that the pyrographite tube with the thermocouples installed on its external, side surface creates a non-intrusive, thermoresistant, and reusable (many times) measuring system, suitable for the discrete detection of combustion zone propagation during the burning of solid high energy materials, *i.e*. in order to determine their average burning rates.

As concerns numerical simulations, these confirmed not only the feasibility of the proposed methodology for burning rate determination of pyrotechnic materials, but they have also proved a good metrological conditioning of the proposed procedure/methodology. In addition, they revealed possibilities for improvement of the measurement procedure by applying more advanced data processing.

5 References

[1] Bahman N.N., *Combustion of Heterogeneous Condensed Systems* (in Russian), *(Goreniye geterogennyh kondensirovannyh sistem)*, Izdatelstvo Nauka, Moskva, **1967**, pp.124-125.

[2] Razdan M.K., Kuo K.K., Erosive Burning of Solid Propellants, in: *Fundamentals of Solid-propellant Combustion*, American Institute of Aeronautics, Inc., New York, **1984**, p.556.

[3] Strunina A.G., Butakova E.A., Demidova L.K., Barzykin V.V., Combustion of Gasless Systems at Cryogenic Temperatures (in Russian), *Fiz. Goreniya Vzryva*, **1988**, *24*(2), 99.

[4] Zarko V.E., Kuo K.K., Critical Review of Methods for Regression Rate Measurements of Condensed Phase Systems, in: *Non-intrusive Combustion Diagnostics,* (Kuo K.K, Parr T., Eds.), Begel House, New York, **1994**, p. 603.

[5] Araujo L., Frota D., Thermochemical Characteristics of AN/AP Based Composite Propellants, *25th Int. Annu. Conf. ICT*, Karlsruhe, Germany, **1994**, 58-1/51-9.

[6] Duraes L., Campos J., Campos-Andrade A., Portugal A., Decomposition Path of Pyrolysis and Combustion of Potassium Nitrate/Thermite Compositions, *IPS Proc. Semin. 33rd*, Fort Collins, CO, USA, **2006**, 232-235.

[7] Dahn C.J., Dastidar A.G., Kashani A., Bradlock M., Brabec T., A New Small-scale Burn Rate Test Method, *IPS Proc. Semin. 33rd*, Fort Collins, CO, USA, **2006**, 291-296.

[8] Hossjer K., Studies of the Heat Problem of Burning Gasless Pyrotechnic Compositions Compressed in Cylindrical Copper-tubes, *Chem. Probl. Connected with the Explos. Stabil., Proc. Symp. 1st*, Stockholm, Sweden, **1967**, 92.

[9] Mordado J., Duraes L., Campos J., Portugal A., Iron Oxide/Aluminum Fast Thermite Reaction using Nitrate Additives, *New Trends Res. Energ. Mater., Proc. Semin., 5th*, Pardubice, Czech Republic, **2002**, 208-222.

[10] Sutton G.P., *Rocket Propulsion Elements*, John Wiley and Sons, Inc., New York, Chapman and Hall Ltd., London, **1956**, pp. 424-425.

[11] *Static Firing Tests of Solid Propellant Rocket Motors*, FR/GE/UK/US International Test Operations Procedures (ITOP) 5-2-500, Defense Technical Information Center (DTIC), **2000**, p. 9, C-1.

[12] Farbisz R., Grudniewicz W., Temperature Measurements of Rocket Motor

Construction Elements (in Polish), *Problemy Techniki Uzbrojenia i Radiolokacji*, **1979**, *20*, 37-47.
[13] Bunker R.C., Ewing M.E., Shipley L., *Pyrolytic Graphite Gauge for Measuring Heat Flux*, US Patent 6499289, **2002**.
[14] Miszczak M., Panas A.J., Swiderski W., A New Method for Continuous Measurements of Solid Rocket Propellant Burning Rate with Use of IR Camera (in Polish), *Pomiary Automatyka Kontrola*, **2009**, *55*(11), 950-953.
[15] Swiderski W., Miszczak M., Panas A.J., A Novel Technique for the Continuous Evaluation of Burning Rate of Solid Rocket Propellant by Using IR Thermography, *QIRT Journal*, **2011**, *8*(1), 111-114.
[16] Miszczak M., Swiderski W., Optical Detection of Combustion Zone Movement in Solid High-energy Materials, *Combust. Explos. Shock Waves*, **2014**, *50*(2), 178-182.
[17] Panas, A.J., IR Support of Thermophysical Property Investigation (Medical and Advanced Technology Materials Study, in: *Infrared Thermography*, (Raghu V.P., Ed.), Intech, Rijeka, **2011**, pp. 65-90.
[18] Panas A.J., Cudziło S., Terpiłowski J., Investigation of Thermophysical Properties of Metal-Polytetrafluoroethylene Pyrotechnic Compositions, *High Temp. – High Press.*, **2003**, *34*, 691-698.
[19] Panas A. J., Panas D., DSC Investigation of Binary Iron-nickel Alloys, *High Temp. – High Press.*, **2009**, *38*, 63-78.
[20] Panas A.J., Cudziło S., Investigations of Temperature Profiles of Deflagration Wave in Me-PTFE Pyrotechnic Mixtures, Temp. and Thermal Measurements, in: *Industry and Science Proc. Symp., 9th*, Cavtat – Dubrovnik, Croatia, **2004**, *2*, 1279-1284.
[21] Melkumov T.M., Melik-Pashaev N.I., Chistiakov P.G., Shiukov A.G., *Rocket Motors* (in Russian), *(Raketnye dvigateli)*, Izdatelstvo Mashinostroeniye, Moskva, **1976**, pp.173-174.
[22] COMSOL *Multiphysics, Heat Transfer Module*, v.33.COMSOL AB, August **2006**.
[23] Ozisk M.N., *Heat Conduction*, John Wiley and Sons Inc., New York, **1993**.
[24] Bejan A., *Convective Heat Transfer*, John Wiley and Sons Inc., New York, **1995**.